CHAPTER 7

Fire Plumes

G. N. MERCER AND R. O. WEBER
School of Mathematics and Statistics, University College UNSW, ADFA Canberra, Australia

I. INTRODUCTION

Ecological studies of the impact of wildland fires need to be concerned with the temperatures to which plants will be subjected. Even though many measurements of the temperatures obtained within and above wildland fires have been made, such as those by Trabaud (1979), to date no one has been able to account for the full variation of temperature with height. Indeed, sampling heights have usually been restricted to less than a few meters and only the plume region above the fire has been modeled. This may suffice for studies of crown death,

Forest Fires
Copyright © 2001 by Academic Press. All rights of reproduction in any form reserved.

such as those conducted by Van Wagner (1973), but it is insufficient for a full understanding of fire effects upon vegetation. Knowing the temperature profile above a fire is important in studying the impact of fire on vegetation. Issues such as leaf scorch, seed death, and stem death all rely on a complete knowledge of the heat exposure of the vegetation.

What is a plume? Anyone who has observed rising smoke or condensed water has seen a plume in action, and anyone considering a fire will immediately realize that the hot gases from that fire will rise and have an impact upon vegetation above the fire (as well as obviously consuming the vegetation in the fire). In broad terms, a plume is characterized by rising buoyant fluids, the buoyancy forces arising from intense localized sources of heat (and/or mass). Comprehensive textbooks on fluid mechanics, such as Yih (1969), or on heat transfer, such as Gebhardt (1971), will contain some discussion of plumes, normally in connection with natural convection above point, line, and plane sources of heat. The discussion will usually focus on the conservation of mass, momentum, and energy and the expression of these conserved quantities as mathematical equations, the Navier-Stokes equations. There are many ways of analyzing the Navier-Stokes equations, including numerical methods (similar to those employed for mesoscale meteorological modeling as in Chapter 8 in this book). Alternatively, it is sometimes possible to derive approximate solutions, which can be very convenient for application to fire situations, particularly when an estimate of the temperatures will suffice. One such approximate solution is a "similarity solution" of the Navier-Stokes equations, where the partial differential equations are simplified by the use of suitable variables, and then the equations can be simplified. The validity of using an approximate solution can be justified by comparison with careful laboratory experiments, which allow one to determine the conditions for which the theory and the phenomena are well understood. Although a valuable technique, similarity solutions will not be used in this chapter, as the mathematical level is more advanced than required for an understanding of the ecological effects of fire. Another, related approximation technique is "dimensional analysis," where the processes involved are considered in terms of the fundamental variables and the dimensions of these variables. Balancing these dimensions can then lead to valuable relationships for quantities of interest, particularly observables such as temperature rise. The most fundamental equation for modeling the ecological effects of fire, Eq. (1), can be derived from dimensional analysis. (In fact, it also arises as a similarity solution of the Navier-Stokes equations with appropriate boundary conditions.) Readers are encouraged to consult the references, such as Yih (1969), for the details of these mathematical techniques.

Early theoretical and experimental work on plumes was conducted during World War II and was inspired by the need to disperse fog from airfields, both in a still atmosphere and in the presence of appreciable wind (see Yih, 1951,

1953; Rouse *et al.*, 1952; Thomas, 1963). Out of this early theoretical and experimental work there arose an understanding that plumes arising from sources of heat only (no mass source at all) could be well described by similarity laws familiar to engineers and scientists (especially in the area of fluid mechanics). The success for both laminar and turbulent flows inspired researchers such as Thomas (1963, 1965) to attempt to use these results to model fire plumes, both in the laboratory and in the field. Van Wagner (1973, 1975) used this model of a fire plume to try to predict scorch heights in forests but only had limited success as the parameters and functional relationships did not turn out as neatly as anticipated. There could be many reasons for this, including the inappropriateness of a plume model with no mass source for modeling a fire or the extended three-dimensional nature of a fire as compared to the idealized line source for the plume model. Whatever the reasons, the landscape fire community was sufficiently "buoyed" by the results to continue trying to gain insight into temperature rise above fires by using relatively simple plume models (e.g., Mercer *et al.*, 1994; Weber *et al.*, 1995a,b).

The most significant relationship for turbulent plumes above line sources of heat (Yih, 1953) can be written as

$$\Delta T = \frac{kI^{2/3}}{z} \tag{1}$$

Here ΔT is the temperature increase above ambient at a height z above the line source of intensity I (measured in power output per unit length). The constant k is a proportionality factor, which Van Wagner (1973) determined from 13 outdoor fires in various forests. If units are used such that ΔT is measured in degrees Kelvin, z is measured in meters, and I is measured in kilowatts per meter, then the constant of proportionality, in SI units, is (M. E. Alexander, 1998):

$$k = 4.47\ Km^{5/3}kW^{-2/3} \tag{2}$$

Naturally this value is not to be used as a "universal constant." Rather it was determined by fitting 13 data points and should only be used as a guide. Furthermore, the two-thirds power of the intensity will not be strictly accurate for the plume above a fire. It also is best used as a guide because it originally arose in a slightly different context and has been adopted for fire plume research in the spirit of elementary mathematical modeling.

A. Alternative Modeling Approaches

Mathematical models of fire plumes can be constructed and presented in a variety of ways. Possibly the simplest is to adopt a relationship such as Eq. (1) and

fit data sets to determine how well the temperature rise is described by such a simple relationship. This empirical approach can be statistically intensive, but it offers the advantage of a well-defined result, hopefully with confidence intervals. For the particular case of Eq. (1), Yih (1953) and Van Wagner (1973), among others, have shown it to provide a reasonable description of turbulent plumes, at least in light wind situations.

An alternative approach is to follow Morton *et al.* (1956); see also Morton (1965) and Williams (1982). This involves a consideration of the main forces affecting the dynamics of a plume and allows one to approximate the equations for conservation of mass, momentum, and energy. The approximate equations can then be solved, usually numerically, and the results expressed graphically. This method can be used to good advantage in more complex situations, such as wind-blown plumes, and will be discussed later in this chapter. The disadvantage is that the final model needs to be implemented in computer software, albeit reasonably simple software, making it a little more cumbersome to use.

The most sophisticated approach is to consider a complete (as far as this is possible) description of the fluid mechanics of a source of heat (and mass) discharging into the atmosphere. This generally involves solving a set of nonlinear, coupled, partial differential equations, the Navier-Stokes equations, and possibly a turbulence model for the fluid motion associated with a fully developed fire plume. Modern computational facilities are quite able to be used efficiently and reasonably quickly to solve problems of this nature; however, it needs to be noted that a great deal of "submodeling" is required and that the end result can really only be used by experts. By submodeling, we mean that the equations as solved have important parameters which need to be pre-determined, the boundaries of the computational domain need to be treated carefully and appropriate conditions must be imposed on fluid velocities and temperature at these boundaries, the source of heat (and mass) must be prescribed in a realistic manner, and the turbulence model must be suitable for a large range of spatial scales including any vegetation on the surface and the full size of the plume. An example of the implementation of such a model is described by Morvan *et al.* (1998), and further examples of this approach can be found in Chapter 8 in this book on coupling atmospheric and fire models. Finally, it should be mentioned that there has been considerable research into plumes in the context of building or structure fires. Some of this can be accessed from the survey paper by Baum (1999) and recent papers such as Trelles *et al.* (1999).

B. Application to Wildland Fires

Fires in the field occur over a large range of environmental conditions, with variations in topography, vegetation, and weather. A proper detailed model would need to be able to account for all of these, at least in principle. Certainly

the comprehensive description of the transport of scalar quantities (such as heat) and vector quantities (such as momentum) will require a full understanding of the fluid flow as it interacts with vegetation. Fundamental studies of this have been completed; see for example the review by Raupach and Thom (1981) or the book by Kaimal and Finnigan (1994). However, the subject of airflow in vegetation has been found to be quite complex, even in the absence of any strong sources of heat and mass such as a fire. For this reason, we must consider the subject of detailed fluid mechanical computations of fire plumes and the interaction with vegetation to be in its infancy.

Consequently, for the remainder of this chapter, we will refrain from very detailed modeling of fire plumes. Rather we shall consider the observables, principally temperature and velocity, and how they are affected by the source strength (fire intensity) and environmental conditions (principally wind). Additionally, we shall consider the impact a particular fire event (rather than a fire regime) can have upon the different sorts of vegetation often encountered in a landscape mosaic.

C. Fire Plume Temperatures

Thermocouple measurements are the primary means for determining temperature rise in and around a fire. Considerable effort has been expended by many researchers (Stocks and Walker, 1968; Trabaud, 1979; Gill and Knight, 1991; Xanthopoulos, 1991) in devising a measurement system which is both robust enough to withstand repeated field work and sensitive enough to give accurate temperature readings. The resolution has relied on a compromise for thermocouple size, with the need for wires to be reasonably strong and also fairly quick to register temperature changes. With an accepted instrument and experimental method, one can then set about the arduous task of gathering temperature data in the laboratory (e.g., Xanthopoulos, 1991), or the field (e.g., Gill and Knight, 1991).

II. MODELING FIRE TEMPERATURE MAXIMA

A. Introduction

In this section we describe a model for the maximum temperature reached as a function of height as a wildland fire passes. The fuel bed, the flaming region above the fuel bed, and the fire plume are all included in the model, but separate temperature–height functions are used in each of the three regions. Continuity of the temperature and the heat flux (through the temperature gradient) across the borders of the regions can then be used to eliminate unnecessary

constants. In this way, it is possible to match a constant-temperature region in the fuel bed with the region of flaming (described by an exponential function characteristic of a reaction-diffusion process) and the classical turbulent plume above the fire.

B. Plume Studies

Yih (1953) calculated the temperatures reached in a turbulent plume resulting from an idealized line source of heat and derived Eq. (1). We note that Eq. (1) is only applicable directly above the stationary source, $x = 0$. Elsewhere, the generalization of this equation, also found by Yih (1953), is

$$\Delta T = \frac{kI^{2/3}}{z} \exp(-x^2/\beta^2 z^2) \tag{3}$$

where x is the horizontal distance from the source and β is an entrainment constant ($\beta \cong 0.16$ according to Lee and Emmons, 1961).

Although, strictly speaking, Yih's (1953) results apply only for a stationary line source in a quiescent atmosphere, Thomas (1963) and subsequently Van Wagner (1973) have used Eq. (1) in modeling the temperature rise above wildland fires. As one reaches a height far above a real wildland fire, it can be reasonably approximated as a line source, and it appears to move only very slowly. Thus, Thomas (1963) and Van Wagner (1973) have had some success—Van Wagner (1973) in particular with providing a first model for crown death.

A laboratory study of stationary pool fires by Kung and Stavrianidis (1982) provides one of the best experimental tests of the applicability of the dimensional analysis of Yih (1953) to fires. The experimental results show impressive agreement in the plume region. However, there is a significant region of measured temperature increases, in and around the flames, where the theoretical results are inadequate.

Our main motivation is to provide a model for the entire temperature profile for wildland fires. The two main benefits of this are

i. The ability to predict maximum external temperature rise to which vegetation would be subjected at any height,
ii. A clarification of the height above a fire at which plume theory can be reliably applied.

Item (i) depends upon the combustion characteristics of fuel types as well as the fluid mechanics of the fire, and we can only provide a partial realization of this here. Item (ii) depends solely upon the fluid mechanics and we show that our model admits an understanding of the significance of the height at which the classical plume theory becomes applicable.

Other factors which one might like to include are the movement of the fire, fire depth, wind profiles, and terrain.

C. Temperature Measurements

The model presented earlier [see Eq. (3)] was fitted to temperature measurements made in a series of experiments in Ku-Ring-Gai National Park near Sydney in New South Wales, Australia. The measurements involved the use of a single vertical array of sheathed Type K (chromel–alumel) thermocouples to measure temperature rises above ambient in experimental fires in heathy fuels. Fires were lit only on days of very light winds. The depth of the fuel varied greatly, from 0.5 to 2 m, and the flames ranged in height from 1 to 10 m. A discussion of the utility of such measurements can be found in Gill and Knight (1991). Typical results are as shown schematically in Figure 1. A detailed report of the experiments is not included here; readers are referred to the detailed report on the experiments, as opposed to the temperature measurements, that can be found in Bradstock and Auld (1995).

It was found that many of the experiments gave a similarity of form, despite quite different fuel depths, which is very encouraging for the development of a

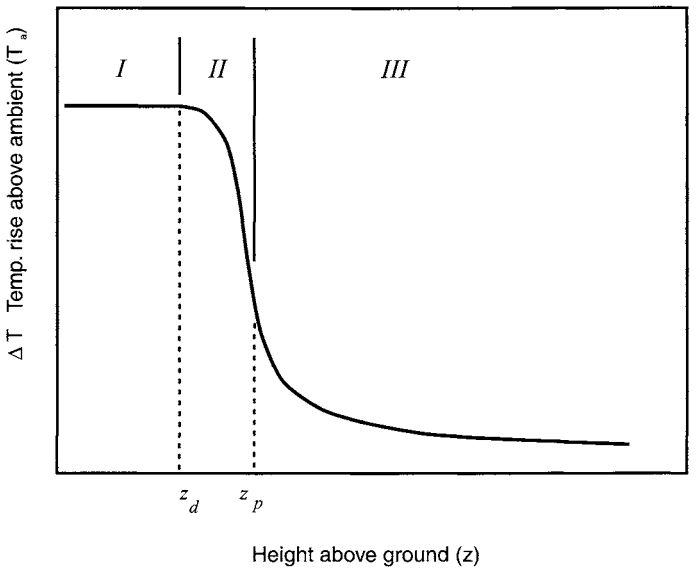

FIGURE 1 Typical form of the curve of the temperature rise above ambient versus the the height above the ground.

universal model. This was the original aim of Thomas (1963) and Van Wagner (1973), founded on the expectation that dimensional reasoning provides relationships which are scale-invariant. The key problem that arose was the inability to determine a universal value for the plume constant [k in Eq. (1)], and indeed there is no reason to expect that in such a simple model k could be a universal constant. In the present analysis, we wish to shift the emphasis away from trying to find universal constants. Rather, it is our expectation that the full temperature versus height profile can be understood with a three-region model, as described in the next two sections with the Ku-Ring-Gai fires as a case study. Furthermore, it will allow a novel comparison of fires and their potential impact upon vegetation.

D. A Three-Region Model

A typical curve of temperature rise above ambient, ΔT, versus height, z, can be divided into three regions, as shown schematically in Figure 1.

$$\text{I:} \quad \Delta T_{\text{I}} = K, \qquad 0 \le z \le z_d \tag{4}$$

$$\text{II:} \quad \Delta T_{\text{II}} = Ke^{-\alpha(z - z_d)^2}, \qquad z_d \le z \le z_p \tag{5}$$

$$\text{III:} \quad \Delta T_{\text{III}} = C/z, \qquad z \ge z_p. \tag{6}$$

where K, C, α, z_d, and z_p are constants which need to be determined. In Region I, it is anticipated that the presence of combusting solid will create a constant high-temperature region which extends through a height z_d, perhaps comparable to the fuel bed depth. In Region II the flames mix with entrained air and an exponential decrease in temperature rise, following a Gaussian distribution, is assumed. Region III is the plume region and extends above a height z_p; hence the plume equation (1) is used (but with the intensity I absorbed into the constant C).

To reduce the number of constants which need to be determined, and to provide a smooth ΔT versus z curve, the temperature rise and the gradient will be matched across the boundaries between regions:

$$\Delta T_{\text{I}}(z = z_d) = \Delta T_{\text{II}}(z = z_d) \tag{7}$$

$$\frac{d}{dz}(\Delta T_{\text{I}})\bigg|_{z=z_d} = \frac{d}{dz}(\Delta T_{\text{II}})\bigg|_{z=z_d} \tag{8}$$

$$\Delta T_{\text{II}}(z = z_p) = \Delta T_{\text{III}}(z = z_p) \tag{9}$$

$$\frac{d}{dz}(\Delta T_{\text{II}})\bigg|_{z=z_p} = \frac{d}{dz}(\Delta T_{\text{III}})\bigg|_{z=z_p} \tag{10}$$

There is a little algebra which needs to be done (see Weber *et al.*, 1995b), but then these conditions determine two of the constants in terms of the other three:

$$C = Kz_p e^{-\alpha(z_p - z_d)^2} \tag{11}$$

$$\alpha = \frac{1}{2z_p(z_p - z_d)} \tag{12}$$

Therefore, the model for ΔT versus z consists of Eqs. (4)–(6) subject to Eqs. (7)–(10). The following three remaining parameters need to be found:

i. K, the maximum temperature reached anywhere. It may be possible to estimate this from a combustion calculation, assuming a certain proportion of total heat generated is lost to the atmosphere.
ii. z_d, perhaps related to fuel bed depth or zone of persistent flame.
iii. z_p, perhaps related to the height of the flames in the zone of flame flickering.

It is valuable to have these guiding roles for K, z_d, and z_p when one comes to fit wildland fire data. A detailed survey of ΔT versus z data from wildland fires is required to fully justify these guiding roles for K, z_d, and z_p. In this context, one should note the extreme paucity of published data which uses thermocouple array or other temperature measurement means. The most detailed studies known to the authors are Tunstall *et al.* (1976), Van Wagner (1975), and Williamson and Black (1981), none of which, in their current form, can be compared with our three-zone model.

E. Fitting Experimental Data

To determine the parameters in the three-region model, seven of the experimental fires are now examined in detail. The three model parameters were first determined approximately by simply viewing the ΔT versus z plots of the experimental data. This instantly provided a smooth curve which gave a good fit to the data. Further refinement using a simple least-squares routine to minimize the error was then done. This usually provided a small improvement to the original fit. In Figures 2 and 3, we present the results of curve fitting from two of the experimental fires. For the fire presented in Figure 2, the fuel bed was quite deep and the flames quite high; hence, we chose $K = 700°C$, $z_d = 1.5$ m, and $z_p = 2.15$ m. For the fire presented in Figure 3, the fuel bed was much shallower, although the flames were of a similar size; hence, we chose $K = 790°C$, $z_d = 0.25$ m, and $z_p = 2.00$ m.

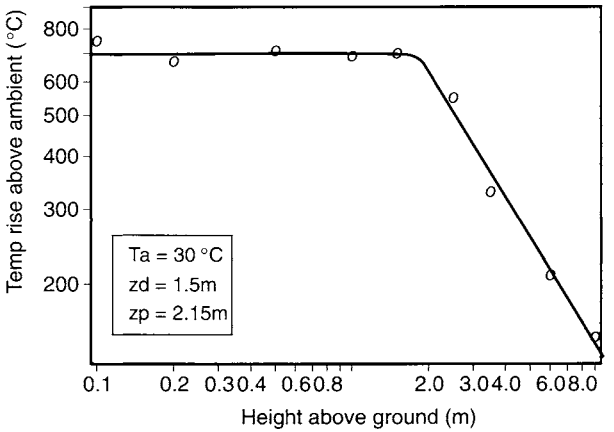

FIGURE 2 Log-log plot of the temperature rise for a deep fuel bed.

The ability of the curves to fit the experimental data with a minimum of fuss is most impressive. It should be stressed that the model is not yet predictive. Indeed detailed measurements in a given fuel type would be required to calibrate the model prior to using it in a predictive sense. Environmental factors such as wind, humidity, and fuel moisture would also need to be taken into account. Despite this, even prior to any calibration, the results provide an insight into where the fire plume region begins. Namely, for the heath communities in Ku-Ring-Gai, NSW, it would seem that 2 m is the minimum height at which plume theory can be successfully applied.

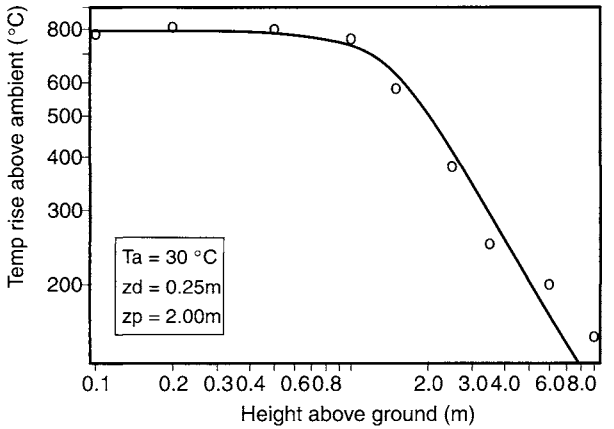

FIGURE 3 Log-log plot of the temperature rise for a shallow fuel bed.

The three regions identified here could match those identified by McCaffrey (1979) for fires burning natural gas above ceramic plates in the laboratory (viz., a continuous-flame region, an intermittent flame region, and a plume region). In wildland fires, the fuel is solid—unlike the fuel in McCaffrey's fires—so it is possible that our regions, especially Region I, may be related to fuel-bed characteristics such as depth. Region I is effectively missing in shallow fuels, such as litter (Stott 1986, author's unpublished data), but readily identified in deeper fuels, such as shrublands (present work and also Trabaud, 1979) and tall grasses (Tunstall *et al.*, 1976). Therefore, the situation described here is a more general one.

F. Time Dependence—Temperature Rise and Fall

Not only is the temperature profile in the plume above a fire of interest, but the temperature–time history is also of critical importance (particularly in regard to vegetation survival). Assuming that a wildland fire is moving at a rate of spread U and that it approximates a line source at position $x = Ut$, then we may recast Eq. (3) as

$$\Delta T = \frac{A}{z} \exp(-t^2/\hat{\beta}^2 z^2) \tag{13}$$

where $\hat{\beta} = \beta/U$, $A = kI^{2/3}$, and $t = 0$ at the time of maximum temperature. Thus, t is negative prior to the arrival of the fire and positive after the fire has passed. This equation gives the temperature rise as the fire approaches but is not valid for the temperature fall.

To determine the temperature fall, note that, from simple Newtonian theory, the cooling rate of a hot object is related to its temperature elevation above ambient by

$$dT/dt = -\gamma(T - T_a) \tag{14}$$

where γ is a constant for a given fuel. Integration of (14) yields the following expression for the ΔT as a function of time:

$$\Delta T = B \exp(-\gamma t) \tag{15}$$

with the obvious condition that B is equal to the ΔT_{max} and thus $B = A/z$ necessarily, where A/z was defined for the temperature rise. This should apply exactly to fires where the combustion residence time is reasonably short. From a fluid-mechanical analysis of the cooling phase, assuming Newtonian cooling, a value for γ of order 0.1 is obtained. This is much greater than values fitted from

experimental data (see discussion that follows) and is thus equivalent to much faster cooling than occurs in practice. The answer to this lies in the fact that real wildland fires leave a trail of partially combusted fuel, from smoldering ash through coals to actively flaming logs; hence, the combustion residence time is not necessarily short. Therefore, γ obtained from a least-squares fit to data from such fires will be an "effective" cooling.

In addition to the experimental fires in Ku-Ring-Gai Chase National Park, near Sydney, data were also fitted using experiments at the CSIRO Kapalga Experimental Station in Kakadu National Park, Northern Territory. The Ku-Ring-Gai fuels were shrublands, varying in depth from 0.5 to about 2 m (Weber *et al.*, 1995b), while the Kapalga vegetation consisted of mainly long dry grass and intermittent shrubs and eucalypts to about 15 m maximum height (Moore *et al.*, 1995). Data from seven Ku-Ring-Gai fires and 20 Kakadu fires, obtained over a 3-year period, were analyzed. Here we choose to only use results at the 3.5- and 6.0-m level above ground since the $1/z$ plume theory is more likely to apply and the moving fire is more like a line source when viewed from that height. Figures 4 and 5 show the results of fitting Eqs. (13) and (15) to one of the Ku-Ring-Gai fires at 3.5 and 6.0 m above ground level, respectively. Both curves were constrained to pass through ΔT_{max}. Note the rapid rise into maximum (within 60 s) after the fire's onset, followed by a slow fall in temperature over more than 300 s following the maximum. However, at large positive values of time, temperatures tend to an elevated level above those predicted by the Newtonian cooling model. This is reflected in the fitted values for the cooling parameter γ

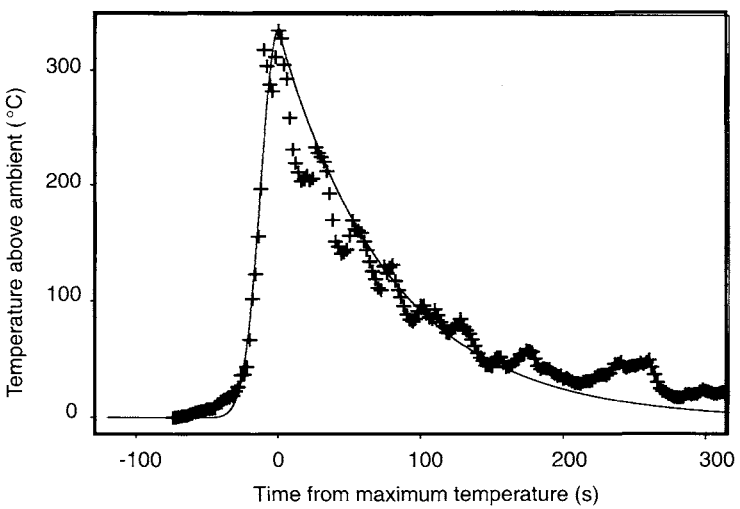

FIGURE 4 Temperature–time curve and data for the Ku-Ring-Gai fire at 3.5 m.

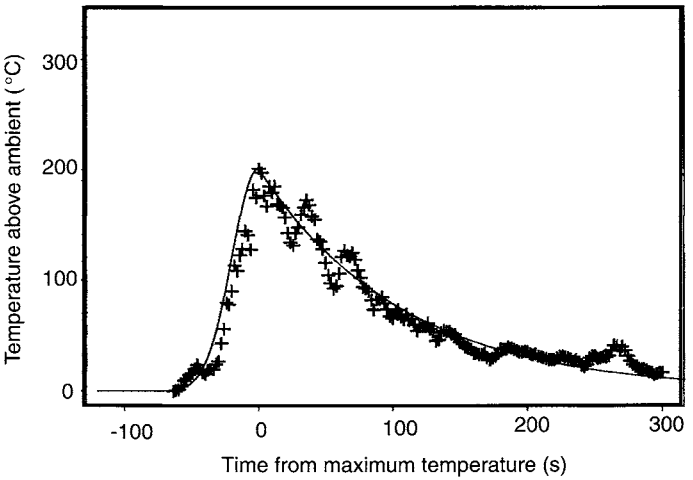

FIGURE 5 Temperature–time curve and data for the Ku-Ring-Gai fire at 6.0 m.

which were 0.013 and 0.009 at the 3.5- and 6.0-m levels, respectively. These are an order of magnitude smaller than the theoretical Newtonian value of about 0.1. The fluctuations in ΔT which occur during cool-down probably correspond to small-scale flaring of fuel elements and also to slow fluid-mechanical phenomena connected with air entrainment. Figures 6 and 7 depict temperatures against time for a Kakadu fire, for 3.5 m and 6.0 m above ground level. The

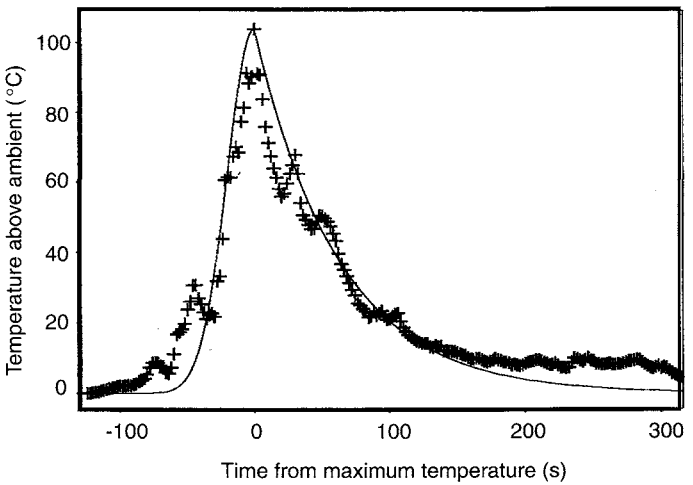

FIGURE 6 Temperature–time curve and data for the Kakadu fire at 3.5 m.

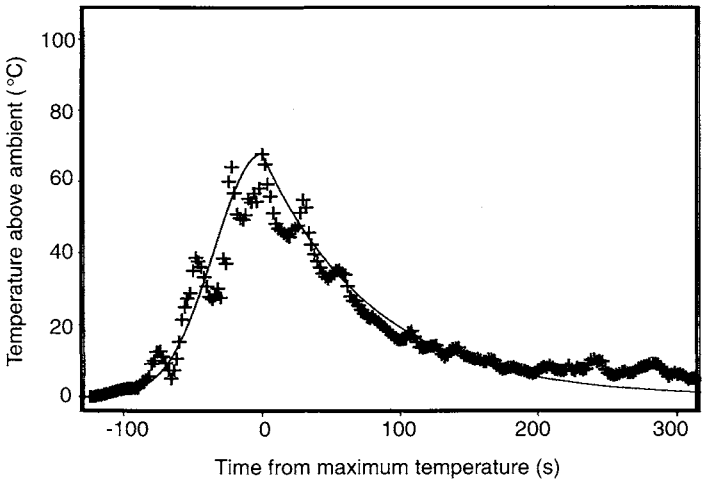

FIGURE 7 Temperature–time curve and data for the Kakadu fire at 6.0 m.

scaling is quite different from that of the Ku-Ring-Gai fire, yet the same qualitative behavior is evident. Again, the model *underpredicts* the decline because it is unable to accommodate prolonged smoldering or persistent combustion after the firefront has passed. The fitted value of γ was 0.016 at 3.5 m and 0.013 at 6.0 m. In both fires, the fit around the model is very good.

G. Total Time-above-Temperature

See also Chapter 14 in this book by Dickinson and Johnson. The simple approach to predicting thermal death of plant materials in fires would be to take the length of exposure above certain temperatures and compare the results with those from constant temperature exposure in a furnace or water bath. Given experimental temperature data or fitted curves such as those in Figures 4–7, the total time for which a given value of ΔT is exceeded may be read directly off the graph. However, with a little algebra, we may express time above ΔT as a function of ΔT as follows: From Eq. (13) the time above ΔT during which the temperature is rising is

$$t_r = \beta z(\ln(A/z\Delta T))^{1/2} \tag{16}$$

From Eq. (15), the time above ΔT during which the temperature is falling is

$$t_f = (1/\gamma)\ln(A/z\Delta T) \tag{17}$$

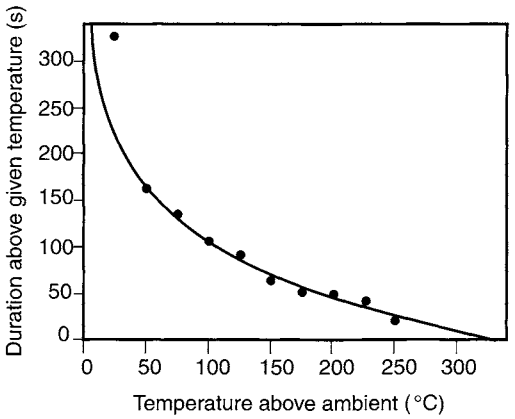

FIGURE 8 Duration of the fire above a given temperature for the Ku-Ring-Gai fire at 3.5 m.

Therefore, the total time above ΔT is

$$t_{tot} = \beta z(\ln(A/z\Delta T))^{1/2} + (1/\gamma)\ln(A/z\Delta T) \tag{18}$$

Fitted values of A, β, and γ were inserted into Eq. (18), and the resulting curves are shown in Figures 8–11.

It is also possible to obtain an estimate of time above ΔT directly from the thermocouple data. This is fraught with problems as it requires an interpolation between data points. However, in order to evaluate our method of fitting temperature–time curves, it seemed appropriate to compare the two methods

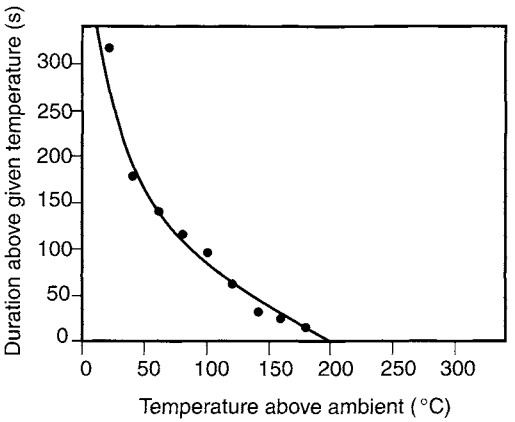

FIGURE 9 Duration of the fire above a given temperature for the Ku-Ring-Gai fire at 6.0 m.

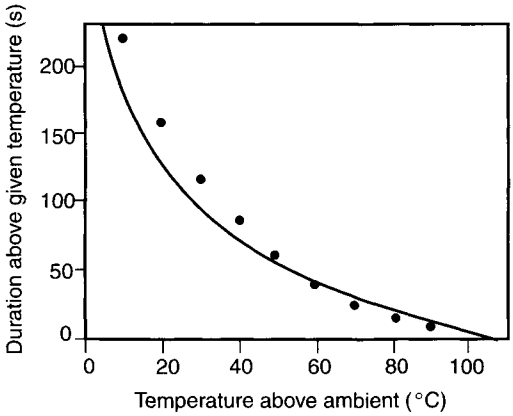

FIGURE 10 Duration of the fire above a given temperature for the Kakadu fire at 3.5 m.

of finding time above ΔT. Hence the "data" points on Figures 8–11 exhibit the same trend as the curve from Eq. (18).

H. Using Time above ΔT to Estimate Death

Laboratory measurements of temperature–time exposures which cause leaf death usually come from bathing the sample in a constant temperature and measuring the time till death (see Chapter 14 in this book for more on this topic). This is not a true representation of the temperature exposure in a fire, due to many factors including the variability in thermal environment associ-

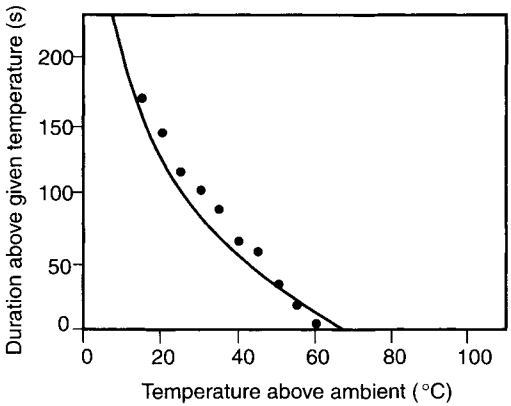

FIGURE 11 Duration of the fire above a given temperature for the Kakadu fire at 6.0 m.

ated with wildland fires and the different thermal properties of water and air but, for obvious reasons, is the convenient experiment to perform. It provides curves like those in Martin *et al.* (1969), characterized by the equation

$$\ln t_d = a - bT \tag{19}$$

where t_d is the time to death at an exposure temperature T.

A way in which these laboratory curves might be used together with our temperature–time relationship [given by Eq. (18)] to predict leaf death and other fire effects follows. It is the heat flux and the ability of the vegetation to dissipate heat that governs the temperature rise of a sample. However, the flux is difficult (if not impossible) to estimate for a given fire, at a given height and time, even with temperature information. Hence, in the absence of detailed understanding of the fluid mechanics, we are forced into considering only the temperature information available to us.

We first notice that the lethal time at a constant temperature, T_{const}, will be more than the lethal time at a varying temperature, $T_{var}(t)$, where the minimum is always equal to or greater than T_{const}. It is then clear that we can perform a direct comparison of the time above a given temperature curve from a fire with the death curves found in the laboratory. This provides a bound on the effects of the fire on vegetation. Namely, if the time–temperature curve is ever at a higher temperature than the death curve, then the vegetation being considered will perish. However, if the death curve is always above the time–temperature curve, we cannot be certain of the fate of the vegetation. These possibilities are shown together in Figure 12.

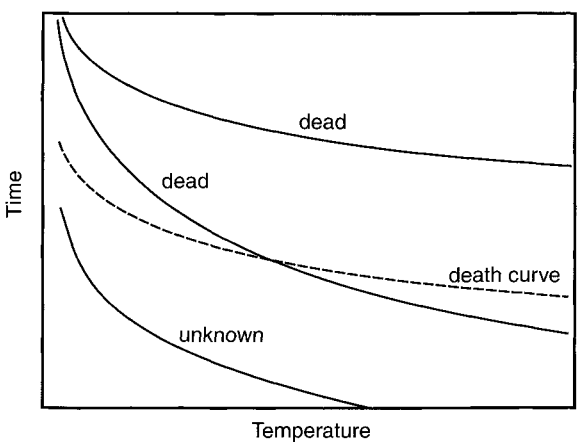

FIGURE 12 A typical death curve and some of the possibilities for the time–temperature curves and the effect on vegetation.

A better method to determine the fate of the vegetation, particularly in this uncertain zone, consists of the following. Divide the time–temperature curve into discrete temperature ranges and determine the time spent within a particular range. The ratio of this calculated time to the laboratory-measured time to death at a representative time in the same range is then determined. This allows for both the heating and cooling phases that the vegetation is subjected to. If we assume additivity of these exposures, then the sum of these ratios will give an indication of the likelihood of death. Mathematically, this can be expressed as a "death number," D,

$$D = \sum_i \frac{t(T_{i-1} < T < T_i)}{t_d(T_i^*)} \tag{20}$$

where $t(T_{i-1} < T < T_i)$ is the time spent in the temperature range (T_{i-1}, T_i) and $t_d(T_i^*)$ is the laboratory measured time to death of a representative temperature (T_i^*) in the range (T_{i-1}, T_i). If the sum of these ratios, the death number (D), is greater than 1, then death is likely, and if the sum is less than 1, then the vegetation is likely to survive. Of course, for values near 1, the outcome is still uncertain. The larger the number, the closer together the discrete temperature ranges considered; hence, the narrower the temperature range, the more accurate this method will be. In the limit as the width of the temperature range tends to zero, Eq. (20) can be rewritten

$$D = -\int_{\tau=T_a}^{T_{max}} \left(\frac{1}{t_d(\tau)} \frac{dt(\tau)}{d\tau} \right) d\tau \tag{21}$$

which, using the model for the external temperature [Eq. (18)] and the model of Martin *et al.* (1969) for the time to death [Eq. (19)], gives the death number as

$$D = \left(\frac{\beta z}{2} + \frac{1}{\gamma} \right) e^{-a} \int_{\tau=T_a}^{T_{max}} \frac{e^{b\tau}}{\tau - T_a} d\tau \tag{22}$$

What is needed are the laboratory-measured time to death of the vegetation (leaves, fruit, stem) for as many different temperatures as possible to determine $t_d(T)$ and the external temperature profile either from experiments or the model detailed previously. The fires considered here both have a maximum temperature well above 60°C; hence, leaf scorch will occur at the heights in question. The effects of fire exposure on the fruits and stems could be determined using the preceding method. Unfortunately, at present, the data needed to use Eq. (20) or to fit to the model of Martin *et al.* (1969) [Eq. (19)] to find $t_d(T)$ are not available in the literature. Mercer *et al.* (1994) have used the model outlined here as the external temperature input to their model for the temperature exposure of seeds in woody fruits. Judd and Ashton (1991) have conducted experimental heating of seeds to consider survival, and Bradstock *et al.* (1994) have examined banksia seed survival during wildland fires. All this work is really the prelimi-

nary stage of these investigations, and there is a need for mathematical modeling and experimental studies to be conducted together to provide reliable methods for predicting the full impact of wildland fires on vegetation.

III. PLUMES ABOVE FIRES IN A CROSS WIND

A. INTRODUCTION

Here a more detailed two-dimensional model of the plume above a line fire is presented by considering the balancing of mass, momentum, and energy associated with the fire and a cross wind. The case where the fire influences the wind profile, which is possible for intense fires, is not considered here. For the sake of this model, the wind profile is an input parameter. This has advantages because different wind profiles such as over grasslands or in tree canopies are easily incorporated. Of interest here is how a cross wind affects the plume above a line fire in both tilting the plume and with increased entrainment into the plume. For a comprehensive approach where the wind profile and fire are coupled, see Chapter 8 in this book.

The previous model was based on the assumption that the wind was light enough that it had little impact on the plume above the fire. Van Wagner (1973) derived correlations for the scorch height of vegetation above a fire in a light wind. This work was based on the assumption that the plume is simply tilted without being distorted and did not take into account the increased entrainment into the plume due to the cross wind. Nevertheless, it was used to try to predict the scorch height for vegetation above wind-blown wildland fires and is an interesting example of a relatively simple correlation model. A model of the wind-blown flame from a line fire was presented by Albini (1981a) who replaced entrainment to the plume velocity (this is the no-wind vertical plume assumption for entrainment) by accretion proportional to the cross-flow velocity. This work concentrated only on the flame and was not extended to the plume above the fire. Fleeter *et al.* (1984) considered Gaussian distributions for the velocity and temperature above the fire and analyzed the case when the cross-wind velocity is comparable to the entrainment velocity.

There have been numerous detailed (but similar) models developed to describe buoyant plumes from point heat sources (often referred to as axisymmetric plumes) in a cross flow (Schatzmann, 1979; Davidson, 1986a,b; Krishnamurthy and Hall, 1987, to name but a few). In contrast, buoyant plumes above a line heat source in a cross flow have had considerably less attention. The model used here is developed in a similar manner to these point heat source (axisymmetric) plume models which are often used to model the discharge from stacks but can also be used to model the plume above a pool fire. The models consist

of a system of coupled ordinary differential equations derived from the conservation of mass, momentum, and energy of the plume. There are generally two types of distribution of velocity and temperature (or density) used in these models: top-hat distributions where the velocity and temperature are considered to be constant across the plume and have the ambient level outside the plume and Gaussian where the velocity and temperature are taken to have Gaussian distributions across the plume. It has been shown by Davidson (1986a) that the differences between the top-hat and Gaussian approaches for the point heat source (axisymmetric) plume are small over the range of parameters of practical interest. The top-hat approach, which requires the solution of a simpler set of equations, will be used here. If more detail than the mean plume behavior (obtained from the top-hat model) is required, then it can be determined by fitting Gaussian distributions from the top-hat results (Davidson, 1986a).

B. Mathematical Formulation

The situation modeled here is an idealization of a blown line fire plume as shown in Figure 13. The plume is considered to be initially rising vertically with velocity w_i, half width b_i, temperature T_i, and density ρ_i. These initial conditions are taken to be far enough above the flames so that the detailed structure of the flame is not required. Values for these initial conditions must be obtained from measurements or from flame models. The ambient atmosphere is at T_a and has density ρ_a and a height-dependent wind velocity $U_a(z)$. Mass entrainment

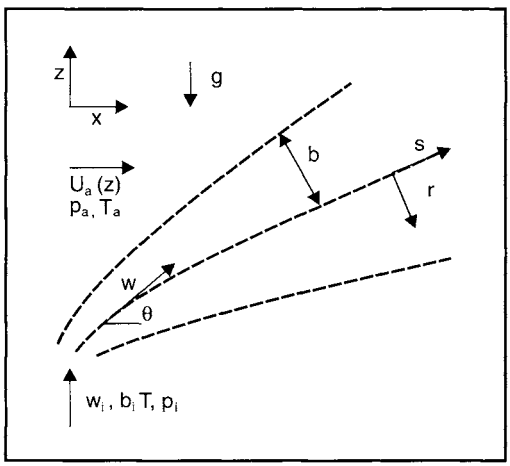

FIGURE 13 A schematic of the plume and cross wind showing the nomenclature used.

of the ambient air into the plume is represented by the linear sum of the horizontal and vertical components. That is, for the plume that is at an angle θ to the flow, the entrainment speed, v_e, is given by

$$v_e = \alpha(w - U_a \cos\theta) + \beta U_a \sin\theta \tag{23}$$

where w is the velocity of the plume. For the case of the axisymmetric plume, values for α and β are documented with $\alpha \approx 0.1$ and $\beta \approx 0.5$ (Krishnamurthy and Hall, 1987). For the line plume, there are less data available in the literature for the value of these parameters, and further measurements are needed to generate reliable estimates for them. Throughout this paper, the value of α will be taken as 0.16 as in Lee and Emmons (1961), and β will have the value 0.5.

In a similar manner to that described in Davidson (1986a) for the axisymmetric plume, the governing equations are derived from balancing the fluxes of momentum and energy. Conservation of mass gives

$$\frac{d(\rho_p b w)}{ds} = \rho_a v_e \tag{24}$$

where s is the arc length along the plume centerline and ρ_p and b are the density and half width, respectively. Due to the top-hat assumption, the density (temperature) and velocity are assumed constant across the width. Conservation of s-momentum gives

$$\frac{d(\rho_p b w^2)}{ds} = \rho_a v_e U_a \cos\theta - b(\rho_p - \rho_a) g \sin\theta \tag{25}$$

Conservation of r-momentum (r is the direction normal to s) gives an equation for the trajectory angle

$$\frac{d\theta}{ds} = -\frac{\rho_a v_e U_a \sin\theta + b(\rho_p - \rho_a) g \cos\theta}{\rho_p b w^2} \tag{26}$$

The conservation of thermal energy gives

$$\frac{d(\rho_p b w T_p)}{ds} = \rho_a v_e T_a \tag{27}$$

where T_p is the plume temperature. Rearranging (27) by using (24) gives

$$\frac{d(\rho_p b w \Delta T)}{ds} = -\rho_p b w \sin\theta \frac{dT_a}{dz} \tag{28}$$

where $\Delta T = T_p - T_a$ is the difference in the temperature of the plume above the ambient air and dT_a/dz is the measure of the temperature stratification in the ambient atmosphere which, for the purposes of this model, can be taken as

zero; that is, here we are considering a neutral atmosphere. This is easily altered if a stratified or unstable atmosphere is to be considered. The ideal gas law gives

$$\rho_p = \rho_a \frac{T_a}{T_p} \tag{29}$$

and the plume trajectory is defined by

$$\frac{dx}{ds} = \cos\theta \tag{30}$$

$$\frac{dz}{ds} = \sin\theta \tag{31}$$

The model then consists of solving the seven equations (24)–(26) and (28)–(31) for the seven unknowns b, w, T_p, ρ_p, θ, x, and z as functions of distance along the plume trajectory subject to the initial conditions

$$\begin{gathered} b = b_i, \qquad w = w_i, \qquad T_p = T_i, \qquad \rho_p = \rho_i, \\ \theta = \pi/2, \qquad x = 0, \qquad z = 0 \end{gathered} \tag{32}$$

Introducing the change of variables

$$\begin{gathered} y_1 = \rho_p b w, \qquad y_2 = \rho_p b w^2, \qquad y_3 = \theta, \\ y_4 = \rho_p b w \Delta T, \qquad y_5 = x, \qquad y_6 = z \end{gathered} \tag{33}$$

and using Eq. (29), the system of equations can be written

$$\frac{dy_1}{ds} = \rho_a v_e \tag{34}$$

$$\frac{dy_2}{ds} = \rho_a v_e U_a \cos y_3 + \frac{y_1 y_4}{y_2} \frac{g \sin y_3}{T_a} \tag{35}$$

$$\frac{dy_3}{ds} = -\frac{\rho_a v_e U_a \sin y_3}{y_2} + \frac{y_1 y_4}{y_2^2} \frac{g \cos y_3}{T_a} \tag{36}$$

$$\frac{dy_4}{ds} = 0 \tag{37}$$

$$\frac{dy_5}{ds} = \cos y_3 \tag{38}$$

$$\frac{dy_6}{ds} = \sin y_3 \tag{39}$$

In this form, it is a straightforward matter to solve this system of six coupled first-order ordinary differential equations subject to the initial conditions given

by Eq. (32) in the appropriate new variables given by Eq. (33). Here the solutions were determined using the NAG (1991) routine D02BBF which integrates a system of first-order differential equations using a Runge-Kutta-Merson method.

To obtain the simplified version for the no-wind case, it is a simple matter of setting $U_a = 0$ and $y_3 = \theta = \pi/2$ in the preceding equations and noting that Eqs. (36) and (38) are no longer relevant because there is no plume angle or horizontal distance to consider. The arc length variable s also then equates to the height above the source that is $z = s$, and Eq. (39) is also not needed.

C. Wind Profile

For the equations of the model to be solved, the wind profile $U_a(z)$ must be specified. One of the strengths of this model is that any horizontal wind profile can be used and hence a variety of conditions can be modeled. For example, the plumes above grassland fires or fires above and below canopies, all of which have different velocity profiles, can each be modeled. In this chapter, no attempt is made to model the impact of the fire upon the prevailing wind field. Near the fire, this is unrealistic because there can be substantial effects upon the wind field due to the fire. However, a much more detailed model that takes into account all of the fluid mechanics and possibly also the combustion properties of the fire would be needed to accurately predict the effect of the fire on the velocity profile (the fluid mechanics is included in the discussion in Chapter 8 in this book).

As a first (somewhat unrealistic) approximation, we consider the wind to be constant with height. This is the situation assumed by Van Wagner (1973) and Fleeter *et al.* (1984). By using a similarity analysis, it has been shown for the uniform wind case that the plume is self-similar (Raupach, 1990); hence, away from the source, the midline trajectory is a straight line as a function of downwind distance, that is $z \propto x$. This agrees with the experimental work of Ramaprian and Haniu (1989) for two-dimensional plumes in a cross-flow. Shown in Figures 14a and 14b are plots of the plume midline trajectory and width for the initial conditions $b_i = 0.2$ m, $w_i = 1.0$ m/s, $T_i = 900$ K with $T_a = 300$ K for $U_a = 1, 3$ m/s, respectively. Clearly, away from the source, the trajectory is a straight line as expected from theory and experimental results. The effect of increasing the wind strength is also evident. With increasing wind strength, the plume is blown over more and hence temperatures at a given height above the heat (fire) are lower as the velocity increases. Therefore, for a fire with a given fixed heat release rate that is independent of the wind strength, vegetation above the fire is exposed to higher temperatures than in a higher wind case. Of course, this does not take into account the effect the wind can have on the heat release rate of the fire.

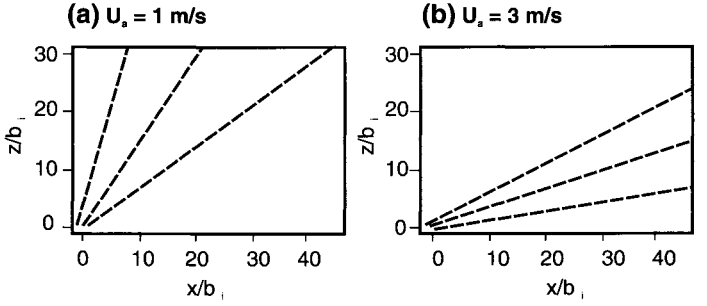

FIGURE 14 Plume trajectory and width for a constant wind.

Two different and more realistic wind profiles are more relevant to the present model. The first is a logarithmic profile as used by Albini (1983), namely,

$$U_a(z) = U_H \frac{\ln\left(\dfrac{z - 0.64V}{0.13V}\right)}{\ln\left(\dfrac{H - 0.64V}{0.13V}\right)} \tag{40}$$

where V is the vegetation height and U_H is the velocity measured at a height H. This velocity profile is applicable above a vegetation cover of trees or shrubs. More applicable to grassland or bare-ground is a power law profile

$$U_a(z) = U_H\left(\frac{z + z_0}{H}\right)^n \tag{41}$$

where n is usually taken as 1/7 (Albini, 1981b, 1983). Here z_0 is the base of the plume and z is measured from this point. Figures 15a and 15b are plots of the plume midline and width for the initial conditions as for Figure 14 but with a

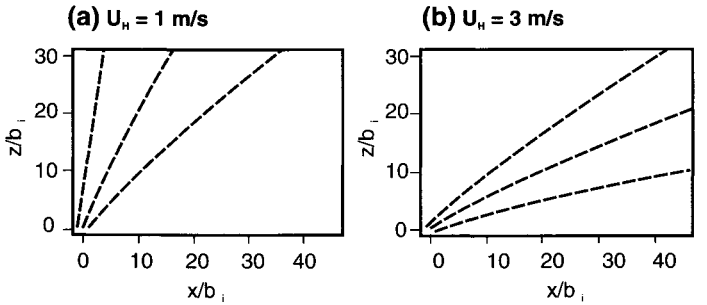

FIGURE 15 Plume trajectory and width for a power law wind profile with U_H given at $H = 10$ m and the plume starting at $z_0 = 1$ m.

power law velocity profile with $U_H = 1, 3$ m/s at $H = 10$ m. The differences between this more realistic profile and the uniform velocity profile considered earlier are evident comparing Figures 14 and 15. The plume for the power law velocity profile is more upright close to the ground as is expected from the lower wind velocities in this region when compared to the uniform velocity case. Far enough above the height where the initial conditions are given, the midline trajectory is approximately linear with downwind distance since the wind velocity is only slowly varying far enough above the source. The major difference between the results for the two different wind profiles is the height to which the plume extends. With a more realistic power law velocity profile, the plume is substantially higher than with a uniform velocity profile. This results in a significant difference when modeling the impact of the fire on vegetation above it and should therefore be taken into account in any such models.

D. Temperature–Time Profiles

Before the effect of the fire plume on vegetation can be determined, the temperature–time profiles at various heights above the fire must be calculated. These temperature–time profiles can then be used as inputs into models for the effect of temperature exposures on vegetation (Mercer *et al.*, 1994). In the present model, the fire is assumed stationary; hence, temperature versus downwind distance profiles can be determined. To convert from this to a temperature–time profile, an estimate must made of the rate of spread of the fire. The distance from the stationary fire can be related to time exposure due to a moving fire. In many circumstances, the rate of spread of fire is small compared to the wind speed; hence, the fact that the fire is moving has little effect on the results presented. In the case when the rate of spread is not small compared to the wind speed, the velocity profile should be altered so that it is relative to the moving fire; that is, the frame of reference should be with the moving fire. In the no-wind case, this is similar to having a wind in the opposite direction to that of the moving fire.

As described in Davidson (1986a), Gaussian distributions can be fitted to the top-hat results of this model to give the distribution within the plume as

$$T_G = T_a + \frac{N}{\lambda^2}(T_p - T_a)e^{-(r^2/\lambda^2 b^2)} \tag{42}$$

where r is the distance normal to the centerline trajectory, N is the plume edge criterion which is usually taken to be 2, and λ^2 is the spreading ratio of mass and heat to momentum which here is taken to be 1 (Davidson, 1986a). Figures 16a and 16b show the temperature versus downwind distance for the

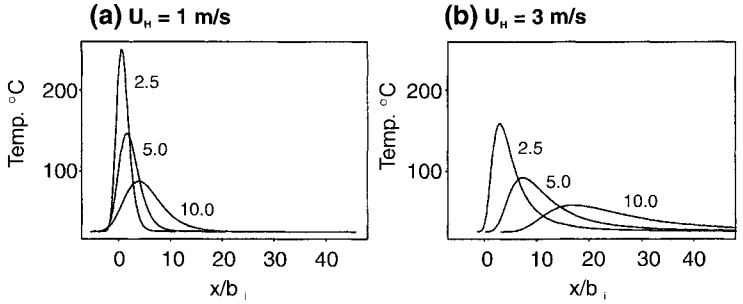

FIGURE 16 Temperature vs. nondimensionalized downwind distance (x/b_i) for the plumes given in Figure 15 at nondimensional heights of z/b_i = 2.5, 5.0, and 10.0.

plumes given in Figures 15a and 15b at three nondimensional heights z/b_i = 2.5, 5.0, 10.0. With increasing wind strength, the maximum temperature reached at any height decreases, and the profiles become more skewed as the plumes are bent over farther. For the lightest wind considered, U_H = 1 m/s, the plume is not far from symmetrical (the no-wind case), whereas for U_H = 3 m/s, there is considerable skewing of the plume downwind.

E. Discussion

This model can be used to predict the temperature–time curves above line fires and hence impact on vegetation above the fire. Certain inputs are needed before the model can successfully be used. The ambient wind velocity profile is needed. This can either be from velocity profiles outlined earlier (or similar analytic profiles) or from measured or predicted velocity profiles depending on the terrain and vegetation involved. Estimates for the initial plume conditions b_i, w_i, and T_i are also required. These can be obtained from either measurements of experimental fires or from models such as the one by Albini (1981a). These will depend on the fire and hence on many parameters such as the fuel type, the loading and moisture content, the wind velocity, the ambient temperature, and the relative humidity to name but a few. Indeed the initial conditions can be related to the heat of the fire

$$Q = \int_{-b_i}^{b_i} C_p w_i \rho_i (T_i - T_a)\, dx \tag{43}$$

which simplifies to

$$Q = 2C_p w_i \rho_i \Delta T_i b_i \tag{44}$$

where $\Delta T_i = T_i - T_a$ is the difference in temperature of the plume from the air. So if an estimate for the heat release rate of the fire is known, then only two of w_i, T_i, or b_i are needed; the third can be estimated from Eq. (44). The most difficult of these initial conditions to determine is w_i, the initial velocity in the plume. The initial plume and temperature are easier quantities to measure experimentally or theoretically from fire models.

The present relatively simple model can be used as an aid in predicting fire impact upon vegetation in many situations. A common reason for using prescribed fire in some parts of the world are fuel reduction burns used to minimize the intensity of wildfires. These have an impact on the surviving vegetation that needs to be estimated before the burns are conducted. Typically fuel reduction burns are conducted in light winds as an aid to their control. They therefore have a larger impact on the vegetation above the fire than a fire of similar intensity would in a stronger wind where the plume is bent farther and does not impinge on the vegetation to such a degree. Of course, the effect of the wind on the fire should also be taken into account. This model can then be used to determine temperature impacts such as the height of scorch of the leaves and potential death of canopy stored seed [in conjunction with models like the one in Mercer *et al.* (1994)].

Since this is only a plume model, no attempt has been made to model the flame of the fire. Models such as the one presented in Albini (1981a) should be used to obtain details of the flaming zone. The present model takes no account of small-scale phenomena such as flare ups; hence, its use is confined to broad areas rather than small areas such as an individual fuel element. Phenomena such as smoldering of fuel after the main fire has passed and the cooling of vegetation and the ground, all of which can possibly increase temperature exposure of the vegetation above the fire, are not considered.

On a larger scale than that considered here, this model can also be incorporated into a model for spotting ahead of a line fire. In this case, the assumption that the atmosphere is neutral is not justifiable; hence, the dT_a/dz term in Eq. (28) should not be taken as zero. An estimate for this temperature stratification in the atmosphere would be needed which would depend upon the atmospheric conditions prevailing at the time. The velocity within the plume has been calculated, and this can be used to determine the height that burning brands will reach before they fall back and possibly ignite a fire downwind of the main fire front. The model presented here differs from previous models of firebrand trajectories in two ways. First, the present model includes the entrainment into the plume due to the cross wind. This is in contrast to existing models for firebrand trajectories (Lee and Hellman, 1969, 1970; Albini, 1979, 1981b, 1983) which use the no-wind assumption that the entrainment velocity is proportional to the vertical velocity. This will overpredict the height to which the firebrand will rise since the plume rises higher in the no-wind case than in

the case with wind present. It is more realistic to include the entrainment as presented in this model in determining the firebrand's actual trajectory. Second, in the present work, a line fire is considered as opposed to previous work by Lee and Hellman (1969) and Albini (1979, 1981b) who considered a spot fire (axisymmetric source) and Albini (1983) who considered a buoyant line thermal as a right elliptical cylinder. The line source is appropriate where the spotting distance is relatively short so that, on the scale of the distance the firebrand has traveled, the fire appears as a line source. For spotting a large distance from the fire, a point source is accurate enough because at a large distance from the fire structure (spot fire or line fire) is less relevant.

NOTATION

Roman Letters

b	plume half width	m
C	constant	m K
C_p	specific heat	J kg^{-1} K^{-1}
g	gravitational acceleration	m s^{-2}
H	height of wind velocity measurement	m
I	line fire intensity	kW m^{-1}
k	constant	K $m^{5/3}$ $W^{-2/3}$
K	constant	K
N	plume edge criterion dimensionless	
n	power law parameter dimensionless	
Q	heat release	W
r	coordinate normal to s	m
s	distance along plume	m
ΔT	temperature rise above ambient	K
T	temperature	K
$U_a(z)$	ambient wind velocity	m s^{-1}
V	vegetation height	m
v_e	entrainment speed	m s^{-1}
w	plume velocity	m s^{-1}
x	horizontal distance	m
z	vertical distance from plume base	m

z_0	height of the plume base	m
z_d	height related to the fuel bed depth	m
z_p	height related to the start of the plume	m

GREEK LETTERS

α	entrainment coefficient	m^{-2}
β	entrainment coefficient dimensionless	
Δ	change from ambient	
λ^2	spreading ratio of mass and heat versus momentum	
θ	plume trajectory angle from the horizontal	
ρ	density	$kg\ m^{-3}$

SUBSCRIPTS

a	ambient property
i	initial property
p	plume property
G	Gaussian

REFERENCES

Albini, F. A. (1979). "Spot Fire Distance from Burning Trees—A Predictive Model." United States Department of Agriculture, Forest Service, General Technical Report INT 56. Intermountain Forest and Range Experimental Station, Ogden.

Albini, F. A. (1981a). A model for the wind-blown flame from a line fire. *Combustion and Flame* **43**, 155–174.

Albini, F. A. (1981b). "Spot Fire Distance from Isolated Sources—Extensions of a Predictive Model." USDA Forest Service Research Note INT 309. Intermountain Forest and Range Experimental Station, Ogden.

Albini, F. A. (1983). Transport of fire-brands by line thermals. *Combust. Sci. Tech.* **32**, 277–288.

Alexander, M. E. (1998). "Crown Fire Thresholds in Exotic Pine Plantations of Australia." PhD thesis. Australian National University.

Baum, H. R. (1999). "Large Eddy Simulations of Fires—From Concepts to Computations." Society of Fire Protection Engineers, 1999 Arthur B. Guise Medal Lecture.

Bradstock, R. A., and Auld, T. D. (1995). Soil temperatures during experimental bushfires in relation to fire intensity: Consequences for legume germination and fire management in south-eastern Australia. *J. Appl. Ecol.* **32**, 76–84.

Bradstock, R. A., Gill, A. M., Hastings, S. M., and Moore, P. H. R. (1994). Survival of serotinous

seedbanks during bushfires: Comparative studies of Hakea species from south-eastern Australia. *Aust. J. Ecol.* **19**, 276–282.

Davidson, G. A. (1986a). Gaussian versus top-hat profile assumptions in integral plume models. *Atmospheric Environment* **20**, 471–478.

Davidson, G. A. (1986b). A discussion of Schatzmann's integral plume model from a control volume viewpoint. *J. Climate Appl. Meteorol.* **25**, 858–867.

Fleeter, R. D., Fendell, F. E., Cohen, L. M., Gat, N., and White, A. B. (1984). Laboratory facility for wind-aided firespread along a fuel matrix. *Combustion and Flame* **57**, 289–311.

Gebhardt, B. (1971). "Heat Transfer." McGraw-Hill, New York.

Gill, A. M., and Knight, I. K. (1991). Fire Measurement. *In* Conference on Bushfire Modeling and Fire Danger Rating Systems (N. P. Cheney and A. M. Gill, Eds.). pp. 137–146. CSIRO Division of Forestry, Canberra.

Judd T. S., and Ashton D. H. (1991). Fruit clustering in the Myrtaceae: Seed survival in capsules subjected to experimental heating. *Aust. J. Bot.* **39**, 241–245.

Kaimal, J. C., and Finnigan, J. J. (1994). "Atmospheric Boundary Layer Flows: Their Structure and Measurement." Oxford University Press, Oxford, UK.

Krishnamurthy, R., and Hall, J. G. (1987). Numerical and approximate solutions for plume rise. Atmospheric Environment **21**, 2083–2089.

Kung, H-C., and Stavrianidis, P. (1982). Buoyant plumes of large-scale pool fires. *In* "19th Symposium on combustion," pp. 905–912. The Combustion Institute (Pittsburgh).

Lee, S-L., and Emmons, H. W. (1961). A Study of natural convection above a line fire. *J. Fluid Mechanics* **11**, 353–369.

Lee, S-L., and Hellman, J. M. (1969). Study of fire-brand trajectories in a turbulent swirling natural convection plume. *Combustion and Flame* **13**, 645–655.

Lee, S-L., and Hellman, J. M. (1970). Fire-brand trajectory study using an empirical velocity-dependent burning law. *Combustion and Flame* **15**, 265–274.

Martin, R. E., Cushwa, C. T., and Miller, R. L. (1969). Fire as a physical factor in wildland management. *In* "Proc. 9th Ann. Tall Timb. Fire Ecol. Conf.," pp. 271–288.

McCaffrey, B. J. (1979). "Purely Buoyant Diffusion Flames: Some Experimental Results." U.S. National Bur. Standards Rep. No. NBSIR 79-1910.

Mercer, G. N., Gill, A. M., and Weber, R. O. (1994). A time dependent model of the fire impact of seeds in woody fruits. *Aust. J. Bot.* **42**, 71–81.

Moore, P. H. R., Gill, A. M., and Kohnert, R. (1995). Quantifying bushfires for ecology using two electronic devices and biological indicators. *CALM Science Supplement* **4**, 83–88.

Morton, B. R. (1965) Modeling fire plumes. *In* "Tenth Symposium (International) on Combustion," pp. 973–982. The Combustion Institute (Pittsburgh).

Morton, B. R., Taylor, G. I., and Turner, J. S. (1956). Turbulent gravitational convection from maintained and instantaneous sources. *Proc. Roy. Soc. (Lond.)* **A234**, 1–15.

Morvan, D., Porterie, B., Larini, M., and Loraud, J. C. (1998). Numerical simulation of turbulent diffusion flame in cross flow. *Combust. Sci. Tech.* **140**, 93–122.

NAG (1991). "Numerical Algorithms Group Fortran Library," Mark 15, Vol. 2. NAG, Oxford, UK.

Ramaprian, B. R., and Haniu, H. (1989). Measurements in two-dimensional plumes in cross flow. *J. Fluids Eng.* **111**, 130–138.

Raupach, M. R. (1990). Similarity analysis of the interactions of bushfire plumes with ambient winds. *Math. Comput. Modeling* **13**, 113–121.

Raupach, M. R., and Thom, A. (1981). Turbulence in and above plant canopies. *Ann. Rev. Fluid Mech.* **13**, 97–129.

Rouse, H., Yih, C. S., and Humphreys, H. W. (1952). Gravitational convection from a boundary source. *Tellus* **4**, 201–210

Schatzmann, M. (1979). An integral model of plume rise. *Atmospheric Environment* **13**, 721–731.

Stocks, B., and Walker, J. (1968). Thermocouple errors in forest fire research. *Fire Technol.* **4**, 59–62.

Stott, P. (1986). The spatial pattern of dry season fires in the savanna forests of Thailand. *J. Biogeog.* **13**, 345–358.

Thomas, P. H. (1963). The size of flames from natural fires. *In* "9th Symp. (Int.) on Combustion," pp. 844–859. The Combustion Institute (Pittsburgh).

Thomas, P. H. (1965). Buoyant diffusion flames: Some measurements of air entrainment, heat transfer and flame merging. *In* 10th Symp. (Int.) on Combustion," pp. 983–996. The Combustion Institute (Pittsburgh).

Trabaud, L. (1979). Etude du comportement du feu dans la garrigue de chêne kermes à partir des températures et des vitesses de propagation. *Ann. Sci. Forest.* **36**, 13–38.

Trelles, J., McGrattan, K. B., and Baum, H. R. (1999). Smoke transport by sheared winds. *Combustion Theory and Modeling* **3**, 323–341.

Tunstall, B. R., Walker, J., and Gill, A. M. (1976). Temperature distribution around synthetic trees during grass fires. *For. Sci.* **22**, 269–276.

Van Wagner, C. E. (1973). Height of crown scorch in forest fires. *Can. J. Forest Res.* **3**, 373–378.

Van Wagner, C. E. (1975). Convection temperatures above low intensity forest fires. *Can. For. Service Bi-monthly Res. Notes* **31**, 21 and 26.

Weber, R. O., Gill, A. M., Lyons, P. R. A., and Mercer, G. N. (1995a). Time dependence of temperature above wildland fires. *CALM Sci. Suppl.* **4**, 17–22.

Weber, R. O., Gill, A. M., Lyons, P. R. A., Moore, P. H. A., Bradstock, R. A., and Mercer, G. N. (1995b). Modeling wildland fire temperatures. *CALM Sci. Suppl.* **4**, 23–26.

Williams, F. A. (1982). Urban and wildland fire phenomenology. *Prog. Energy Combust. Sci.* **8**, 317–354.

Williamson, G. B., and Black, E. M. (1981). High temperature of forest fires under pines as a selective advantage over oaks. *Nature* **293**, 643–644.

Xanthopoulos, G. (1991). "A Model for the Prediction of Crowning in Forest Fires." PhD thesis. University of Montana.

Yih, C. S. (1951). Free convection due to a point source of heat. *In* "Proc. 1st U.S. Nat. Congre. Appl. Mech.," pp. 941–947.

Yih, C. S. (1953). Free convection due to boundary sources. *In* "Fluid Models in Geophysics," Proc. First Symposium on the use of Models in Geophysics, pp. 117–133. U.S. Gov't Printing Office, Washington.

Yih, C. S. (1969). "Fluid Mechanics." McGraw-Hill, New York.